

# Open-Vocabulary Camouflaged Object Segmentation

Youwei Pang<sup>1,2\*</sup>, Xiaoqi Zhao<sup>1,2\*</sup>,  
Jiaming Zuo<sup>2</sup>, Lihe Zhang<sup>1\*\*</sup>, and Huchuan Lu<sup>1</sup>

<sup>1</sup> Dalian University of Technology

<sup>2</sup> X3000 Inspection Co., Ltd

{lartpang,zxq}@mail.dlut.edu.cn

klaus@3000gy.com, {zhanglihe, lhchuan}@dlut.edu.cn

**Abstract.** Recently, the emergence of the large-scale vision-language model (VLM), such as CLIP, has opened the way towards open-world object perception. Many works have explored the utilization of pre-trained VLM for the challenging open-vocabulary dense prediction task that requires perceiving diverse objects with novel classes at inference time. Existing methods construct experiments based on the public datasets of related tasks, which are not tailored for open vocabulary and rarely involve imperceptible objects camouflaged in complex scenes due to data collection bias and annotation costs. To fill in the gaps, we introduce a new task, open-vocabulary camouflaged object segmentation (OVCOS), and construct a large-scale complex scene dataset (**OVCamo**) containing 11,483 hand-selected images with fine annotations and corresponding object classes. Further, we build a strong single-stage open-vocabulary camouflaged object segmentation transformer baseline **OVCoser** attached to the parameter-fixed CLIP with iterative semantic guidance and structure enhancement. By integrating the guidance of class semantic knowledge and the supplement of visual structure cues from the edge and depth information, the proposed method can efficiently capture camouflaged objects. Moreover, this effective framework also surpasses previous state-of-the-arts of open-vocabulary semantic image segmentation by a large margin on our OVCamo dataset. With the proposed dataset and baseline, we hope that this new task with more practical value can further expand the research on open-vocabulary dense prediction tasks. Our code and data can be found in the [link](#).

**Keywords:** Open Vocabulary · Camouflaged Object Segmentation

## 1 Introduction

The ability to identify and reason about object regions in a visual scene is essential for a wide range of human activities. As a complex and fundamental task in

---

\* Equal Contribution.

\*\* Corresponding Author.

computer vision, detecting and segmenting objects with diverse appearances in complex scenes is also an important challenge, which is crucial for applications across vision and robotics fields, including autonomous driving [3], medical image analysis [35], and intelligent robotics [90], to name a few. In the past few years, numerous typical methods [6, 7, 19, 75] have emerged with the help of a mass of labeled data, which have greatly promoted the development of related fields such as semantic image segmentation (SIS) [11, 57]. However, existing works have mainly focused on predefined closed-set scenarios, where all semantic concepts are seen during both the inference and training phases. Such a scenario setting oversimplifies the real-world complexity. To this end, many explorations have been contributed to open vocabulary settings [60, 89]. In existing work, open vocabulary learning utilizes visual-related language data (e.g., object class text or descriptions) to align images and language features, enabling models to perceive novel classes without extensive labeled data [60]. Recently, large-scale pre-trained visual language models (VLMs) such as CLIP [9, 50] have been gaining attention. Image-text matching-based learning mechanism provides them with the ability to align textual and visual signals well, and many works demonstrate their potential for open vocabulary tasks. Besides, data plays an important role in open-vocabulary tasks. Existing open-vocabulary semantic image segmentation (OVSIS) tasks rely on related public datasets [4, 12, 43, 44, 85], while they are not designed for the open-vocabulary setting, and there is high semantic similarity between their class definitions as revealed in [63]. Due to the data collection bias and annotation cost constraints, the existing open-vocabulary benchmarks lack special attention to finely perceive the objects of interest in concealed scenes. And the widely used VLMs are pre-trained on image-text pairs with inherent object concept bias, thus, their ability to segment objects in complex scenes remains to be verified.

In this paper, we introduce a new open-vocabulary segmentation task OVCOS dedicated to analyzing camouflaged object perception in diverse natural scenes. And a large-scale data benchmark, named OVCamo, is carefully constructed. Besides, we also design a strong baseline OVCoser for the proposed OVCOS, based on the VLM-driven single-stage paradigm. The camouflage<sup>3</sup> arises from several sources, including similar patterns to the environment (e.g., color and texture) and imperceptible attributes (e.g., small size and heavy occlusion) as statistically illustrated in Fig. 3. Considering the imperceptible appearance of camouflaged objects, accurate recognition

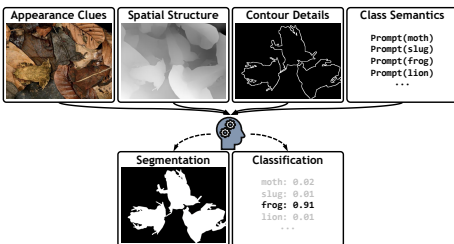


**Fig. 1:** The perception and recognition of camouflaged objects require the collaboration of information from multiple sources such as appearance clues, spatial structure, contour details, and object semantics.

<sup>3</sup> To ensure the reliability of the definition, we follow existing published literature and collect data from the *class-agnostic* camouflage perception field, i.e., CSU [15].



small and clean public datasets, which limits their achievable performance, and their fine-tuning on specific downstream tasks hinders application flexibility. In [42], image-text pairs collected from the Internet bring clear performance improvement for the retrieval task. This also indirectly encourages subsequent further exploration, such as CLIP [9, 50]. It benefits from the larger scale of noisy data from web pages covering diverse and rich concepts and exhibits impressive open-vocabulary capabilities. This work introduces CLIP as the bedrock of open-vocabulary capability and borrows its strong image-text matching capability to build an effective baseline for the OVCOS task.

**Open Vocabulary Semantic Image Segmentation (OVSIS).** Although a variety of pipelines have emerged as summarized in [89], from an overall perspective, their efforts are similar, namely, *how to align class name/description semantic embedding with visual features to anchor relevant object cues in the representation space*. The early pioneer work [76] attempts to connect word concepts and semantic relations, and encodes word concept hierarchy to parse images. Due to the leading performance of the VLM on the image-text joint modeling, it has been gradually applied in the OVSIS field. In terms of structure, existing schemes can be roughly categorized into two types: two-stage [33, 62, 64, 71] and single-stage [10, 70, 86]. In [71], a rough segmentation map for each class is created from a VLM and then refined by the test-time augmentation. These rough maps are utilized as pseudo-labels for subsequent fine segmentation by stochastic pixel sampling. SimSeg [64] adopts a cascaded design including class-agnostic proposal generation by MaskFormer [7] and class assignment by CLIP [50]. Furthermore, OVSeg [33] fine-tunes CLIP on the noisy but diverse data to improve its generalization to masked images. In lieu of using existing SIS models, a text-to-image diffusion model is introduced to generate mask features with implicit image captions in [62]. The single-stage design is more flexible and simpler. MaskCLIP [86] directly modifies CLIP for semantic segmentation without training, while SAN [63] achieves better performance with the help of adapters. CAT-Seg [10] highlights the importance of the cost aggregation between image and text embeddings for the OVSIS decoding. Recent FC-CLIP [70] investigates the hierarchical CLIP image encoder. Although these methods show impressive OVSIS performance, they still follow the generalized segmentation paradigm [6, 7] in SIS, ignoring valuable auxiliary cues for object perception. This also causes them to struggle with objects camouflaged in complex scenes. Unlike them, our method, which is tailored for OVCOS, can effectively tap into the camouflaged object by integrating task-specific multi-source knowledge from visual appearance, spatial structure, object contour, and class semantics.

**Camouflaged Scene Understanding (CSU).** This is a research hotspot in the computer vision community, aiming to perceive objects with camouflage [15]. Different from traditional object perception like salient object detection [22, 23, 30, 31, 45, 48, 49, 69, 72–74, 78–83] and semantic object segmentation [21, 77], CSU is obviously a more challenging problem. It can be applied in some specific fields, such as medical analysis [13, 16] and agricultural management [36, 52]. This topic is currently defined as the class-agnostic form, fo-

cusing on the area of camouflaged objects in the visual scene. The available work [8, 13, 14, 24, 28, 46, 47, 68] to date has demonstrated promising performance on existing data benchmarks [2, 8, 14, 27, 40, 54]. Unlike previous settings, the proposed OVCOS task requires further perception of object classes. Admittedly, the publicly available data provides critical support for this new task. It helps us take the first step.

### 3 OVCamo Dataset

This work focuses on open-vocabulary segmentation in the camouflaged scene. It enriches the connotation of OVSIS and provides a more challenging benchmark. Note that our aim is not to claim novelty through class annotations alone, but rather to focus on how such annotations can pave the way for new tasks and methods. Our dataset provides additional features such as clean data, less ambiguity, and sensible class hierarchies, which provide the necessary data for solving the new and complex task. It not only adds complexity and challenge, but also promotes innovation and advances the field through the need for advanced methods. We believe that this dataset can lead to new opportunities in areas such as wildlife conservation and intelligence sensing.

**Image Collection.** Our data is collected from existing CSU datasets that have finely annotated segmentation maps. Specifically, the OVCamo integrates 11,483 hand-selected images covering 75 object classes reconstructed from several public datasets [2, 8, 14, 65, 84]. The distribution of the number of samples in different classes is shown in Fig. 2. Meanwhile, we consider attributes of

objects when selecting images, such as object concentration, average color ratio, object-image area ratio, number of object parts, and normalized centroid. Tab. 1 gives their definitions. And Fig. 3 visualizes the attribute distribution of the proposed dataset. The camouflaged objects of interest usually have complex shape Fig. 3a, high similarity to the background Fig. 3b, and small size Fig. 3c. And the image often contains multiple camouflaged objects or sub-regions with a central bias as shown in Figs. 3d and 3e.

**Annotation.** The original annotation cannot be used directly in the open-vocabulary setting, due to the following semantic ambiguities caused by different annotation standards, *i.e.*, 1) Broad concepts, such as “fish” and “bug”; 2) Vague definitions, such as “small fish” and “black cat”; 3) Inconsistent granularity, such as the coexistence of “orchid mantis” and “mantis”; 4) Non-entity concepts, such as “other”. These issues can lead to unreasonable and unreliable results for the open-vocabulary prediction as discussed in [87]. To this end, we relabel the classes of all camouflaged objects and take the generality of

**Table 1:** Attributes involved in the dataset analysis.

Attribute	Description
Object Concentration	Object pixel concentration, which calculates the area ratio between the object region and its minimum rotatable bounding box.
Average Color Ratio	Color ratio of the object to the background, which calculates the average of the three color channels in their respective regions.
Object-Image Area Ratio	Area ratio of the object relative to the image.
Number of Object Parts	Number of separate areas in the image that belong to the object.
Normalized Centroid	Object centroid coordinates, which are normalized using the image shape.

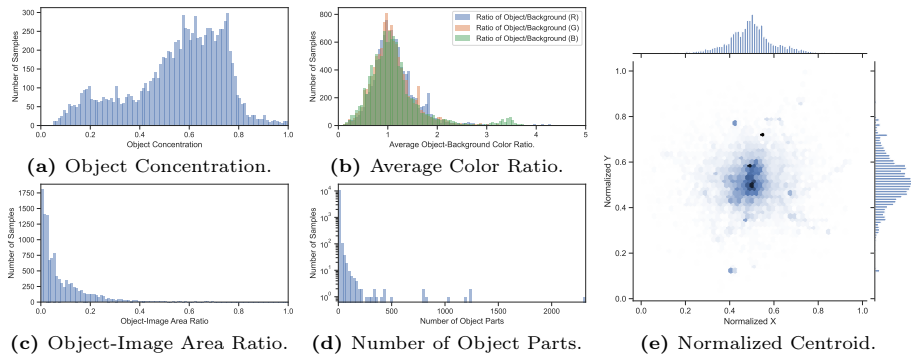


**Fig. 3:** Attribute visualization of objects in our OVCamo dataset, including object concentration, object-background color ratio, object-image area ratio, number of object parts, and normalized centroid. Please refer to Tab. 1 for details about attributes.

the concept as the criterion for class definition, which also ensures lower semantic similarity. The similarity analysis and rough hierarchy of the class set  $\mathcal{C}$  can be found in Appendix B.

**Data Division.** To objectively evaluate the open-vocabulary segmentation algorithm on unseen classes, we assign as many classes as possible to the test set and control the sample ratio of the training set to the testing set to be 7:3. Specifically, 14 classes in the dataset are taken as the training set and all the remaining 61 classes are used for testing. Such a setting follows the existing practice in OVSIS where the number of seen classes (*e.g.*, 171 [4]) is usually fewer than unseen classes (*e.g.*, 847 [85]) which is also closer to the real-world setting. Such a setup can ensure the quantity of training samples while reinforcing the complexity of the test set. Finally, the overall ratio of samples is 7713:3770.

## 4 Methodology

In this section, we introduce a strong baseline OVCoser. The overall framework is first described, followed by the details of the key components.

**Overall Architecture.** We follow the common encoder-decoder paradigm and the pipeline is shown in Fig. 4. Specifically, we first leverage the textual encoder  $\mathbf{E}_t$  of the frozen CLIP to extract semantic embedding  $f_t$  from the class label set  $\mathcal{C}$ , and the visual encoder  $\mathbf{E}_v$  to extract multi-scale image features  $\{f^i\}_{i=1}^5$ . Both of them are fed into the decoder as the information bedrock of object segmentation, as shown in Fig. 5. Structural cues such as depth and edge are also introduced to assist the iterative refinement process. Finally, the class-related segmentation  $P_s$  which is the segmentation logits  $M_s$  after the `sigmoid` function processing, is used to remove the interference from the background in the high-level image feature and guide the generation of object-oriented visual representation  $f_v$ . And the class label  $P_c$  is determined by the similarity matching between  $f_v$  and  $f_t$ . More details about the proposed architecture are listed in Appendix A.

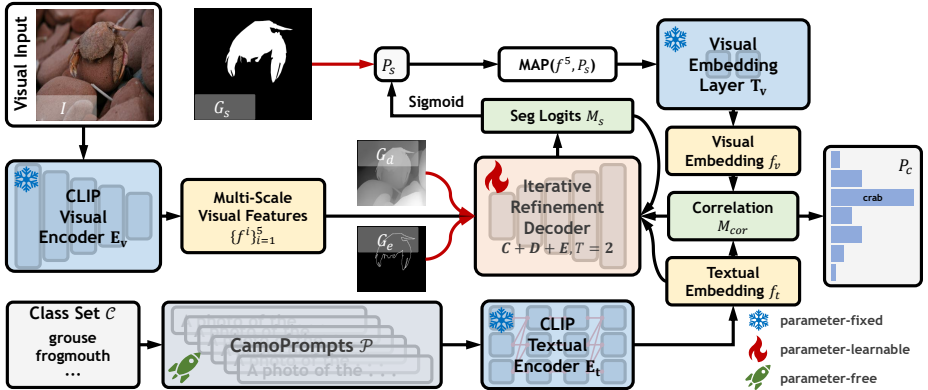


**Fig. 4:** Overview of our single-stage open-vocabulary camouflaged object segmentation framework, OVCOSer. It is based on the frozen CLIP model which includes feature encoder  $E_v$  and embedding layer  $T_v$  for visual appearance cues and textual encoder  $E_t$  for class semantic information. The well-constructed prompt template set CamoPrompts  $\mathcal{P}$  enables textual embedding  $f_t$  to be more appropriate to OVCOS. In the iterative refinement decoder (Fig. 5), a more accurate class-related segmentation  $P_s$ , can be obtained with the assistance of the semantic guidance  $C$  (Fig. 6a) from the class semantic and the structure enhancement (Fig. 6b) from the auxiliary depth and edge supervisions, *i.e.*,  $D$  and  $E$ . After being masked average pooled (MAP) by  $P_s$ , the high-level feature  $f^5$  is used to assign a class  $P_c$  to the object from the class set  $C$ . Note that  $D$  and  $E$  are only used as auxiliary supervision during training and are not required during inference.

**Semantic Guidance (SG).** The class label definition usually is independent of the image scene. It is very important to fully utilize the class prior for object recognition in complex scenes. In the proposed decoder, normalized textual embedding is introduced into each stage to highlight semantically relevant cues. As shown in Fig. 6a, we design a semantic guidance component SG to inject concept cues into the self-enhancement of the image feature. Specifically, in our **semantic guidance attention (SGA)**, the normalized image feature  $X$  is linearly mapped to  $Q$ ,  $K$ , and  $V$ , while the textual embedding  $f_t$  is transformed to the class guidance vector  $G_t$ . The similarity between  $Q$  and  $G_t$  reflects the activation of different classes in spatial locations. In **Agg** of Fig. 6a, the base weight  $W_b$  for the spatial guidance is obtained after highlighting the most relevant class information by **softmax** operation. And then  $V$  is modulated and fed into **MHSA**, *i.e.*, multi-head self-attention [59].

**Structure Enhancement (SE).** Existing methods demonstrate that low-level structural information, such as the edge [56] and the depth [61], plays an important role in CSU, which is closely related to the mechanism of the human visual system. So the SE component attached to the low-level SG is proposed to integrate the edge-aware and depth-aware cues and improve the structural details. Specifically, the output of the SG is fed into two separate branches containing the convolutional stem and head for the edge and depth estimation as shown

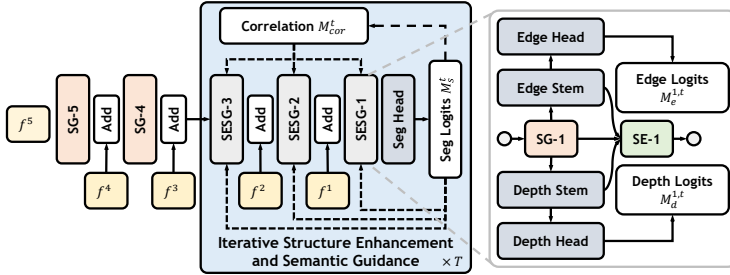


**Fig. 5:** Proposed pipeline of the iterative refinement decoder with semantic guidance (SG) and structure enhancement (SE) components denoted as “SG- $\star$ ” and “SE- $\star$ ”.  $t$  and  $T$  denote the current step and total number of iterations, respectively.

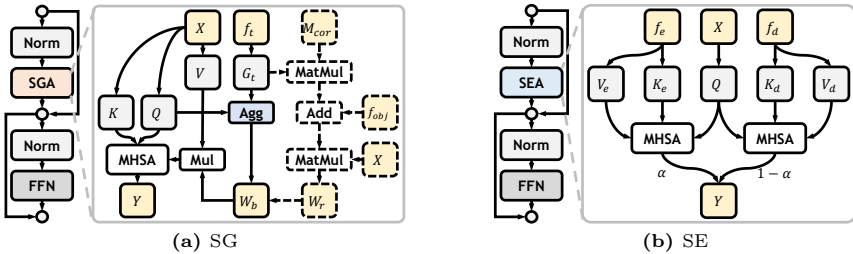


**Fig. 6:** Proposed semantic guidance (SG) and structure enhancement (SE) components in which semantic guidance attention (SGA) and structure enhancement attention (SEA) are embedded. The dashed blocks represent the feedback paths that come into play during iteration.

in Fig. 5. The edge and depth logits maps, *i.e.*,  $M_e^i$  and  $M_d^i$ , from the head in the branch of the layer  $i \in \{1, 2, 3\}$  are directly supervised. And the outputs  $f_e^i$  and  $f_d^i$  of the stem are fed into the SE. In the **structure enhancement attention (SEA)**, they independently update the normalized visual features  $X$  using MHSA [59], and the corresponding outputs are combined with the learnable weight  $\alpha$  as in Fig. 6b.

**Iterative Refinement.** In the SG component, the aggregation process between image features and class semantics is not aligned and requires data-driven optimization. Considering the aligned embedding space of the pre-trained CLIP, we introduce the correlation matrix  $M_{cor}$  between the visual and textual embeddings into the SG as shown in Fig. 6a. Meanwhile, due to the emphasis of the decoder output on the object region, the object-aware representation  $f_{obj}$  is also inputted, which comes from the image features pooled by the coarse segmentation prediction in the last iteration. By combining the two, we obtain task-oriented object cues, which is actually inspired by the top-down attention mechanism in the human cognitive system [1, 25]. The spatial activation map  $W_r$  of such object cues over image features is used to re-modulate  $W_b$ . Besides, the SE in the iteration also helps the model to further optimize the texture details. To benefit as much as possible from the assistance from structure enhancement

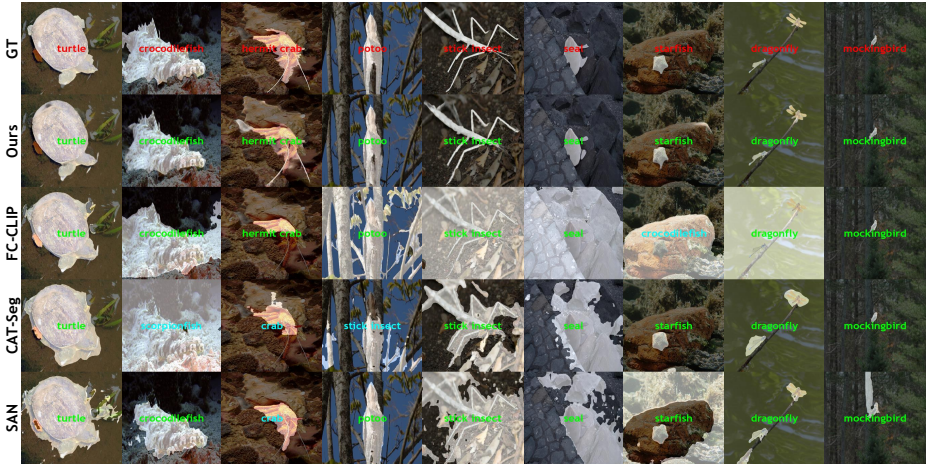


**Fig. 7:** Visual results on OVCamo. Existing methods are either disrupted by chaotic backgrounds, imperceptible appearances, blurry details, or severe occlusion, while our algorithm can effectively capture and remain well-exposed object details. And three different colors are used to represent **human annotations**, **correct predictions**, and **incorrect predictions**.

while avoiding over-computation, we set the iteration entry to the third decoding layer as shown in Fig. 5.

**CamoPrompts.** As mentioned in [50], prompt engineering and ensembling are important for the transfer performance of CLIP on downstream tasks, and the prompt template should be more relevant to the data type. Because additional task-related cues are generally able to impose the necessary contextual constraint to the flexible CLIP. Hence, instead of common practices [18, 50, 88], we design a simpler yet more effective template set CamoPrompts tailored for OVCOS to decorate the class name, and average their textual embeddings as the final semantic embedding for each class. Its full form is depicted in Tab. 4, while it also achieves better classification performance in comparison with other forms.

**Supervision.** In each iteration, in addition to semantic object segmentation, we also need to perform depth estimation and edge estimation as auxiliary tasks. For the segmentation prediction, we follow the commonly used weighted segmentation loss function  $l_s^t = l_s(P_s^t, G_s)$  [56, 68]. For the edge estimation, considering the imbalance problem of positive and negative samples, we introduce the dice loss function as  $l_e^{i,t} = l_e(P_e^{i,t}, G_e)$ . The summation of L1 and SSIM losses, *i.e.*,  $l_d^{i,t} = l_d(P_d^{i,t}, G_d)$ , is used for the depth estimation. The total loss  $L$  of our method can be formulated as follows:  $L = \sum_{t=1}^T \left[ l_s^t + \sum_{i=1}^3 \left( l_e^{i,t} + l_d^{i,t} \right) \right]$ , where  $t$  and  $i$  are used to index iterations and layers, respectively. And the total number  $T$  of iterations is set to 2 as mentioned in Sec. 5.3.

## 5 Experiments

### 5.1 Implementation Details

**Dataset Settings.** As mentioned in Sec. 3, the proposed dataset is divided according to classes into two disjoint subsets, *i.e.*,  $\mathcal{C}_{seen}$  and  $\mathcal{C}_{unseen}$ . The former contains 14 classes for training and the latter contains the remaining 61 classes for testing. The proposed dataset itself is provided with only images and masks. We use the typical monocular depth estimation methods [26, 51] to obtain the depth map  $G_d$  for training, while the edge map  $G_e$  is generated by dilating and eroding operations. *We introduce depth and edge maps only in the training phase and they are not required during inference, which also avoids information leakage during testing.* So, our depth and edge maps are labor-free and training-only, and directly generated by existing algorithms. Such a design can help our model get rid of the dependence on them in real-world applications. Our structure enhancement based on depth and edge information belongs to a deeper exploration of this task. These generated depth maps will be made publicly available with the dataset.

**Training Details.** Following previous settings in [63, 64, 70], the pre-trained CLIP is frozen during training, and the remaining parameters are learnable and are randomly initialized. The AdamW [39] optimizer with the learning rate of  $3e-6$ , weight decay of  $5e-4$ , batch size of 4, and training epoch of 30 is used to optimize model parameters. Some basic data augmentations including random flipping, rotating, and color jittering, are introduced to preprocess training data. The input data and the output logits are bilinearly interpolated to  $384 \times 384$  during training and inference.

**Evaluation Protocol.** To reasonably evaluate the performance of OVCOS, we modify the metrics in the original CSU task [8, 13] to  $cS_m$ ,  $cF_\beta^\omega$ ,  $cMAE$ ,  $cF_\beta$ ,  $cE_m$ , and  $cIoU$  which follows the common settings in the OVSIS field [10, 33, 63, 64, 70, 89] and takes into account both classification and segmentation.

### 5.2 System-level Comparison

To show the complexity of the proposed OVCOS task and also to verify the effectiveness of the proposed method, we compare OVCoser with several recent state-of-the-art methods in OVSIS, including [10, 33, 62–64, 70]. Since this is a new task, existing methods need to be re-evaluated to understand their generalization ability. Based on the public code and weights trained on COCO-Stuff [4] provided by the authors, we show the performance of these methods under three different testing schemes, including S.I) testing directly with their trained weights; S.II) further fine-tuning based on trained weights before testing; and S.III) testing after re-training directly on our training set.

**Quantitative Evaluation.** For the sake of fairness in comparisons, we report the performance of the “Large” versions for these methods, except for SimSeg [64] where the authors only provide the “Base” version. All results are summarized in Tab. 2 and our approach consistently outperforms these competitors. It is

**Table 2:** Comparison with recent state-of-the-art CLIP-based open-vocabulary semantic image segmentation methods with different training settings on the proposed OVCamo dataset. The best three results are highlighted in **red**, **green** and **blue**.

Model	VLM	Feature Backbone	Text Prompt	cS <sub>m</sub> ↑	cF <sub>β</sub> <sup>sw</sup> ↑	cMAE ↓	cF <sub>β</sub> ↑	cE <sub>m</sub> ↑	cIoU ↑
<i>Test on OVCamo with the weight trained on COCO.</i>									
SimSeg <sup>21</sup> [64]	CLIP-ViT-B/16 [50]	ResNet-101 [20]	Learnable [88]	0.128	0.105	0.838	0.112	0.143	0.094
OVSeg <sup>22</sup> [33]	CLIP-ViT-L/14 [50]	Swin-B [37]	[18]	0.341	0.306	0.584	0.325	0.384	0.273
ODISE <sup>23</sup> [62]	CLIP-ViT-L/14 [50]	StableDiffusionv1.3 [53]	[17]	0.409	0.339	0.500	0.341	0.421	0.302
SAN <sup>23</sup> [63]	CLIP-ViT-L/14 [50]	ViT Adapter [18]	[18]	<b>0.414</b>	<b>0.343</b>	<b>0.489</b>	<b>0.357</b>	<b>0.456</b>	<b>0.319</b>
CAT-Seg <sup>23</sup> [10]	CLIP-ViT-L/14 [50]	Swin-B [37]	[50]	<b>0.430</b>	<b>0.344</b>	<b>0.448</b>	<b>0.366</b>	<b>0.459</b>	<b>0.310</b>
FC-CLIP <sup>23</sup> [70]	CLIP-ConvNeXt-L [9]	—	[18]	0.374	0.306	0.539	0.320	0.409	0.285
<i>Finetune on OVCamo with the weight trained on COCO.</i>									
SimSeg <sup>21</sup> [64]	CLIP-ViT-B/16 [50]	ResNet-101 [20]	Learnable [88]	0.098	0.071	0.852	0.081	0.128	0.066
OVSeg <sup>22</sup> [33]	CLIP-ViT-L/14 [50]	Swin-B [37]	[18]	0.164	0.131	0.763	0.147	0.208	0.123
ODISE <sup>23</sup> [62]	CLIP-ViT-L/14 [50]	StableDiffusionv1.3 [53]	[17]	0.182	0.125	0.691	0.219	0.309	0.189
SAN <sup>23</sup> [63]	CLIP-ViT-L/14 [50]	ViT Adapter [18]	[18]	0.321	0.216	0.550	0.236	0.331	0.204
CAT-Seg <sup>23</sup> [10]	CLIP-ViT-L/14 [50]	Swin-B [37]	[50]	0.185	0.094	0.702	0.110	0.185	0.088
FC-CLIP <sup>23</sup> [70]	CLIP-ConvNeXt-L [9]	—	[18]	0.124	0.074	0.798	0.088	0.162	0.072
<i>Train on OVCamo.</i>									
SimSeg <sup>21</sup> [64]	CLIP-ViT-B/16 [50]	ResNet-101 [20]	Learnable [88]	0.053	0.049	0.921	0.056	0.098	0.047
OVSeg <sup>22</sup> [33]	CLIP-ViT-L/14 [50]	Swin-B [37]	[18]	0.024	0.046	0.954	0.056	0.130	0.046
ODISE <sup>23</sup> [62]	CLIP-ViT-L/14 [50]	StableDiffusionv1.3 [53]	[17]	0.187	0.119	0.700	0.211	0.298	0.167
SAN <sup>23</sup> [63]	CLIP-ViT-L/14 [50]	ViT Adapter [18]	[18]	0.275	0.202	0.612	0.220	0.318	0.189
CAT-Seg <sup>23</sup> [10]	CLIP-ViT-L/14 [50]	Swin-B [37]	[50]	0.181	0.106	0.719	0.123	0.196	0.094
FC-CLIP <sup>23</sup> [70]	CLIP-ConvNeXt-L [9]	—	[18]	0.080	0.076	0.872	0.090	0.191	0.072
Ours	CLIP-ConvNeXt-L [9]	—	CamoPrompts	<b>0.579</b>	<b>0.490</b>	<b>0.336</b>	<b>0.520</b>	<b>0.616</b>	<b>0.443</b>

worth noting that existing methods perform better at S.I. This may be attributed to the training process on the larger-scale COCO-Stuff dataset, which provides a more general understanding of the concepts. However, direct fine-tuning (*i.e.*, S.II) may destroy this knowledge and even cause oblivion to some extent, resulting in performance degradation. If we follow S.III to re-train them, the relatively small-scale training data may not be enough to train these models with more complex structures. At the same time, the existing methods also lack targeted optimization for the OVCOS task. These problems can lead to further deterioration of performance. However, our approach tailored for OVCOS achieves leading performance by the iterative refinement strategy of multi-source information, which comprehensively considers different characteristics of the task.

**Qualitative Evaluation.** We also visualize the results of some recent methods on a variety of data in Fig. 7. It can be seen that the proposed method shows better performance and adaptability to diverse objects, including large objects (Col. 1-2), middle objects (Col. 3-5), small objects (Col. 6-9), multiple objects (Col. 8), complex shapes (Col. 3-5), blurred edges (Col. 1-5), severe occlusion (Col. 6), and background interference (Col. 2-6).

### 5.3 Analysis and Ablation Study

**Better Baseline Model.** Interestingly, our baseline model in Tab. 3 outperforms existing methods in Tab. 2. We attribute this to the fact that the overly complex feature pipeline of the conventional OVSIS architecture is not well adapted to this task. And our framework, from hyperparameter setting to struc-

**Table 3:** Ablation comparison of proposed components.  $\Delta$  represents the *average relative gain* in performance of the corresponding model over the baseline for OVCOS.  $\mathcal{P}$ : CamoPrompts.  $\mathcal{C}$ : Semantic guidance.  $\mathcal{D}$ : Depth estimation auxiliary task.  $\mathcal{E}$ : Edge estimation auxiliary task.  $T$ : Number of iterations which is set to 2 by default due to the best performance. “ $\limsup_{P_s \rightarrow G_s} \text{Perf.}$ ”: The ideal performance for our framework.

Model	cS <sub>m</sub> ↑	cF <sub>β</sub> <sup>ω</sup> ↑	cMAE ↓	cF <sub>β</sub> ↑	cE <sub>m</sub> ↑	cIoU ↑	Δ
<i>Comparison of the proposed modules.</i>							
Baseline	0.517	0.408	0.374	0.451	0.549	0.359	0.0%
+ $\mathcal{P}$	0.543	0.435	0.346	0.480	0.581	0.383	6.3%
+ $\mathcal{P}, \mathcal{C}$	0.550	0.453	0.341	0.491	0.597	0.397	9.1%
+ $\mathcal{P}, \mathcal{C}, \mathcal{D}$	0.565	0.473	0.336	0.507	0.606	0.422	12.6%
+ $\mathcal{P}, \mathcal{C}, \mathcal{E}$	0.567	0.481	0.339	0.511	0.607	0.432	13.5%
+ $\mathcal{P}, \mathcal{C}, \mathcal{D}, \mathcal{E}$ ( <i>i.e.</i> , $T = 1$ )	0.570	0.488	0.338	0.518	0.610	0.436	14.5%
SE (Fig. 6b) → Addition Fusion	0.552	0.457	0.340	0.497	0.599	0.402	9.9%
<i>Comparison of the proposed iterative refinement.</i>							
$T = 1$	0.570	0.488	0.338	0.518	0.610	0.436	14.5%
$T = 2$	<b>0.579</b>	<b>0.490</b>	0.336	<b>0.520</b>	<b>0.616</b>	<b>0.443</b>	<b>15.5%</b>
w/o $M_{cor}$ as in Fig. 6a	0.575	0.487	0.337	0.515	0.611	0.441	14.8%
w/o $f_{obj}$ as in Fig. 6a	0.571	0.476	0.339	0.506	0.608	0.434	13.4%
$T = 3$	0.576	0.484	<b>0.333</b>	0.514	0.614	0.437	14.8%
$\limsup_{P_{seg} \rightarrow G_{seg}} \text{Perf.}$	0.703	0.703	0.297	0.701	0.701	0.701	51.2%

tural evolution, is explored for the proposed task and data. Thus, we actually provide a more effective and robust baseline setup for OVCOS.

**Importance of Modules.** To specifically analyze the effect of different components, we evaluate their performance in Tab. 3. As can be seen, the proposed modules all show positive gains. Both the semantic guidance in the class-aware decoding and the structure enhancement from auxiliary tasks of depth and edge estimation consistently boost the final performance. The ablation comparison also demonstrates that explicit guidance of the spatial and contour information is important for the detection of camouflaged objects and their positive gains are subject to the effective fusion design. We replace the proposed structure enhancement (SE) component with the vanilla addition fusion with a similar number of parameters, which results in detrimental effects. Besides, in Tab. 3, we also give the ideal results of our CLIP-driven framework where  $G_s$  is treated as  $P_s$ . Although our method exhibits leading performance compared to existing methods as shown in Tab. 2, there is still a long way to go to solve this problem. At the same time, *the current ideal performance is still far from the limit, suggesting that future breakthroughs in this field may require more powerful paradigms* as discussed in Appendix C.

**Importance of Iterative Refinement.** The top-down iterative refinement strategy significantly improves the OVCOS performance as shown in Tab. 3. When the number  $T$  of iterations is 2, our algorithm obtains the best OVCOS performance. As  $T$  increases, there is no further improvement in performance, so it is set to 2 by default. In addition, the object-aware representation  $f_{obj}$

**Table 4:** Classification accuracy  $\mathcal{A}$  of the plain CLIP using different prompt templates on OVCamo, which is based on the masked average pooling with the ground truth mask.

ID	Prompt Template	$\mathcal{A}$
0	"<class>" w/o MAP based on ground truth	0.538
<i>Task-generic templates.</i>		
1	"<class>"	0.671
2.1	"The <class>."	0.648
2.2	"the <class>."	0.632
2.3	"A <class>."	0.677
2.4	"a <class>"	0.675
3.1	"A photo of a <class>."	0.684
3.2	"A photo of the <class>."	0.691
3.3	"The photo of a <class>."	0.672
3.4	"The photo of the <class>."	0.680
3.5	"a photo of a <class>"	0.684
3.6	"a photo of the <class>"	0.689
3.7	"the photo of a <class>"	0.675
3.8	"the photo of the <class>"	0.674
4	templates from [50]	0.686
5	templates from [18]	0.682
<i>Task-related templates.</i>		
6.1	"A photo of the camouflaged <class>."	0.681
6.2	"A photo of the concealed <class>."	0.674
6.3	6.1, 6.2	0.685
6.4	"A photo of the <class> camouflaged in the background."	0.684
6.5	"A photo of the <class> concealed in the background."	0.694
6.6	6.4, 6.5	0.694
6.7	"A photo of the <class> camouflaged to blend in with its surroundings."	0.700
6.8	"A photo of the <class> concealed to blend in with its surroundings."	0.697
6.9	6.7, 6.8	0.703
6.10	6.1 - 6.9 i.e., CamoPrompts	0.704

from the output space plays an important role, and introducing the correlation guidance  $M_{cor}$  also has positive gains.

### Importance of CamoPrompts.

Our prompt template set CamoPrompts, which takes task attributes into account, shows better performance in Tab. 4. To further understand the influence of different templates on the semantic embedding, we calculate the Hausdorff distance between training and testing class labels in the embedding space, as shown in Fig. 8. The figure presents an interesting phenomenon that those templates with better classification performance tend to reduce the distance, which inspires further explorations for more effective prompt engineering.

### Importance Between Edge and Depth.

In the proposed SE as shown in Fig. 6b, the interaction components for the edge and depth are combined by a coefficient vector  $\alpha$ , which can also reflect the relative importance of the two kinds of information. In Fig. 9, we plot  $\alpha$  from different decoding layers. It can be seen that the values are usually greater than 0.5, which indicates a preference for the edge information flow.

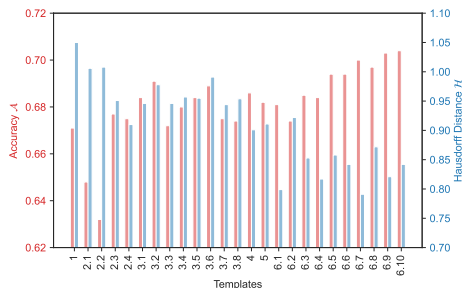


**Fig. 8:** Illustration of classification accuracy  $\mathcal{A}$  and Hausdorff distance  $\mathcal{H}$  between the textual embeddings of training and testing class splits by using the plain CLIP on the OVCamo dataset. The approximate negative correlation between them may reveal that the templates that bring training and testing class embeddings closer usually also improve classification accuracy. Tab. 4 shows the details of these templates.

**Table 5:** Efficiency comparison with other methods. “Trainable Param.” and “Total Param.” stand for the number of trainable and total parameters. In OVSeg [33], the CLIP [50] model is fine-tuned by the authors, resulting in more trainable parameters.

Model	Trainable Param.	Total Param.	FLOPs
SimSeg <sup>21</sup> [64]	61M (28.91%)	211M	1.9T
OVSeg <sup>22</sup> [33]	531M (100.00%)	531M	8.0T
ODISE <sup>23</sup> [62]	28M (1.80%)	1522M	5.5T
SAN <sup>23</sup> [63]	9M (2.06%)	437M	0.4T
CAT-Seg <sup>23</sup> [10]	104M (21.22%)	490M	0.3T
FC-CLIP <sup>23</sup> [70]	20M (5.38%)	372M	0.8T
Ours	7M (1.95%)	359M	0.2T

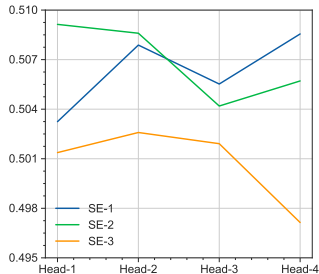


**Fig. 9:**  $\alpha$  corresponding to different heads in Fig. 6b from different decoding layers.

**Model Complexity.** We compare the proposed method with the CLIP-based competitors [10, 33, 62–64, 70] in terms of the number of trainable and total parameters, and FLOPs. To be fair, we test all methods following the setting of their original inference settings. As can be seen from Tab. 5, our method has fewer trainable parameters ( $< 2\%$ ) and less computational complexity ( $0.2T$ ), which is superior to these competitors.

## 6 Conclusion

In this work, we propose a new challenging task, OVCOS, to explore open-vocabulary semantic image segmentation (OVSIS) for the camouflaged objects in more complex natural scenes, and carefully collect and construct a large-scale data benchmark OVCamo. Meanwhile, by considering the characteristics of the task and data, we propose a strong single-stage baseline OVCoser with the advanced pre-trained vision-language model. Specifically, the well-designed prompt templates are introduced to reinforce the task-relevant semantic context. We introduce additional multi-source information including class semantic cues, depth spatial structure, object edge details, and top-down iterative guidance from the output space. With the help of these components, OVCoser can perceive and segment camouflaged objects in complex environments. Extensive experiments demonstrate the effectiveness of the proposed method and its superior performance compared with the existing state-of-the-art OVSIS algorithms on OVCamo.

**Acknowledgements.** We sincerely thank these authors of the public datasets [2, 8, 14, 65, 84] used in this work: Deng-Ping Fan, Ge-Peng Ji, Guolei Sun, Ming-Ming Cheng, Jianbing Shen, and Ling Shao for COD10K [14], Yunfei Zheng, Xiongwei Zhang, Feng Wang, Tiejong Cao, Meng Sun, and Xiaobing Wang for CPD1K [84], Jinyu Yang for PlantCamo [65], Pia Bideau and Erik Learned-Miller for CAD [2], and Xuelian Cheng, Huan Xiong, Deng-Ping Fan, Yiran Zhong, Mehrtash Harandi, Tom Drummond, and Zongyuan Ge for MoCA-Mask [8]. It is their efforts that underpin this new exploration of camouflaged object segmentation.

## A Model Details

### A.1 Details of $\mathbf{E}_v$ and $\mathbf{T}_v$

In the proposed model, the visual encoder  $\mathbf{E}_v$  and embedding layer  $\mathbf{T}_v$  together are used to extract the high-level embedding corresponding to the object of interest in the input image. The two independent sub-networks are split from the visual network of CLIP [9, 50].  $\mathbf{E}_v$  contains all the feature encoding layers for extracting the multi-scale image features. And  $\mathbf{T}_v$  corresponds to the final high-dimensional projection layer, which is used to convert the high-level image feature  $f^5$  into the visual embedding vector  $f_v$ .

### A.2 Multi-scale Image Features $\{f^i\}_{i=1}^5$

The multi-scale image features  $\{f^i\}_{i=2}^5$  is from the four stages of ConvNeXt [38] with different output resolutions, respectively. While the feature  $f^1$  is obtained by up-sampling the feature  $f^2$   $2\times$  by bilinear interpolation.

### A.3 Class Embedding

In the proposed algorithm, for each image input, the textual encoder needs to extract text embedding for all class texts. However, due to the nature of the algorithm design, these text embeddings are shared in each iteration, so they can be pre-computed in the inference to save inference cost.

### A.4 Details of Classification

During the inference, the class prediction  $P_c$  is generated from the pair-wise correlation matrix  $M_{cor}$  after the softmax operation, where  $M_{cor}$  is from the multiplication between the normalized visual embedding and textual embedding, *i.e.*  $f_v$  and  $f_t$ . Besides, in our experiments, introducing classification supervision on top of the existing form interferes with the training process of the model, which brings about significant performance degradation, with relative reductions of 8.6% and 15.7% for  $cS_m$  and  $cF_\beta^\omega$ , respectively. Therefore, we do not consider classification loss during training, and  $M_{cor}$  is only used to construct the top-down iterative guidance.

## B Dataset Details

### B.1 Class Semantic Similarity

To analyze the semantic similarity between the relabelled classes, we compute the path similarity between the classes based on the Open English WordNet [41] as shown in Fig. 10. Specifically, when  $p$  is the length of the shortest path between two classes, the path similarity score  $s$  is:

$$s = \frac{1}{p + 1} \quad (1)$$

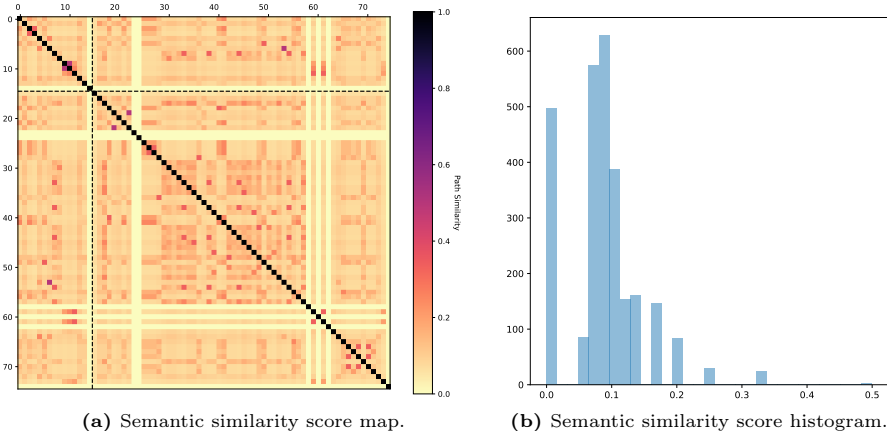


**Fig. 10:** Class semantic similarity of OVCamo based on the Open English WordNet [41]. The classes belonging to the training and testing sets are separated here using black dashed lines in (a). Note that only the similarity between two different classes is considered in (b).

The score  $s$  ranges between 0.0 and 1.0, where the higher the score is, the more similar the two classes are. The score  $s$  is 1.0 when a class is compared to itself, and 0.0 when there is no path between the two classes (i.e., the path distance is infinite). As shown in Fig. 10b, the semantic similarity between classes in our class set  $\mathcal{C}$  is very low. Most of them lie around 0.1, while the maximum is only 0.5. Such low similarity can better alleviate the complexity due to class semantic similarity during open vocabulary evaluation.

## B.2 Class Hierarchy Relationships

In Fig. 11, we use the alluvial graph to show the class relationships at different levels, including super, base, and sub-classes. The sub-classes shown here include class names with clearer meanings preserved from the original data and class names after initial manual correction. The base classes represent the class names obtained after careful manual filtering and merging, which was used in all the experiments in this paper. The super classes generalize the base classes from a broader perspective.

## C Limitations and Future Works

### C.1 Class Embedding Setting

In our proposed algorithm, the class embedding setting follows the existing OV-SIS methods. Although our iteration process does not impose much computational burden due to our caching mechanism, there is still a computational

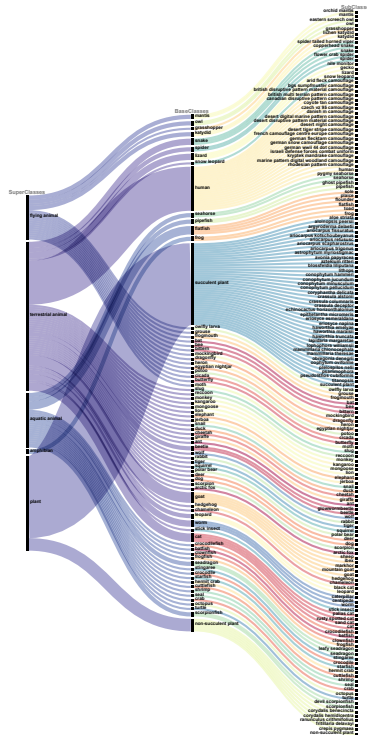


**Fig. 11:** Hierarchy of sample classes contained in the proposed OVCamo. **Only the base classes are used in our experiments.** Sub-classes that do not meet the criteria are simply removed and are not displayed here.

complexity associated with the number of classes. This is not ideal for practical applications in open vocabulary scenarios. More flexible and efficient class embedding designs are still worth exploring.

## C.2 CLIP-based Architecture

The transfer application of the CLIP in downstream dense prediction tasks is limited by its pre-training form and the camouflage scenes that we focus on may be more affected. Some work [10, 33, 63] attempts to further finetune CLIP, but the finetuning strategy still needs to be designed more carefully due to the potential disruption to the CLIP’s open vocabulary ability. And it also suggests that there is room for further improvement. Besides, as mentioned in the main text, the current ideal performance of the CLIP-based architecture is still far from the limit, which suggests that future breakthroughs in this field may require more powerful paradigms.

### C.3 Data Scale

Although the number of finely labeled samples in our proposed dataset is over ten thousand, the data scale is still smaller than existing large datasets such as COCO-Stuff [4] and ADE20K [85]. So there is still a need to collect more data, especially for classes with fewer samples. We can resort to rich web images, which also may lead to significant manual labeling costs. In addition, the data synthesis technique has been demonstrated in some recent work [66,67] to greatly facilitate the performance of semantic image segmentation tasks. This technique based on object masks and textual descriptions in existing datasets, may bring some new insights. But this also needs to address the ensuing interference problem.

### C.4 Class Scale

Open-vocabulary segmentation as a hot topic, currently focuses on how to use the open-vocabulary capability of VLMs to segment objects with unseen classes. More data classes will indeed facilitate the development of OVCOS. However, the imperceptibility of camouflaged objects poses a great challenge for further expansion. This is the focus of our future work.

### C.5 Prompt

The importance of prompt engineering for visual language modeling can be reflected in the existing literature [10, 18, 33, 50, 62–64, 70] and the experiments in this paper. The prompt forms used in this paper rely heavily on manual design, which is still limited by the knowledge of the prompter. More automated prompt-generation strategies may be needed in the future, which deserve more attention and exploration.

## D Dataset Copyright

We have investigated the copyright information of these data sources, and they are currently now widely used in the CSU field [15], and available for non-commercial academic use. Much of existing work [34, 58] provides only new annotations and an index of the original data rather than the data itself. And users can download original data from the sources. Following these existing community practices, for the proposed OVCamo dataset, we list the data links provided by the original authors in the documentation. We also provide the class annotations we created and a detailed description of the way the data is organized in OVCamo. In addition, we thank the contributors of the relevant datasets in the our acknowledgements.

## References

1. Anderson, P., He, X., Buehler, C., Teney, D., Johnson, M., Gould, S., Zhang, L.: Bottom-up and top-down attention for image captioning and visual question

- answering. In: Proceedings of IEEE Conference on Computer Vision and Pattern Recognition (2018) [8](#)
2. Bideau, P., Learned-Miller, E.: It's moving! a probabilistic model for causal motion segmentation in moving camera videos. In: Proceedings of European Conference on Computer Vision (2016) [5](#), [14](#)
  3. Caesar, H., Bankiti, V., Lang, A.H., Vora, S., Liong, V.E., Xu, Q., Krishnan, A., Pan, Y., Baldan, G., Beijbom, O.: nuscenes: A multimodal dataset for autonomous driving. In: Proceedings of IEEE Conference on Computer Vision and Pattern Recognition (2020) [2](#)
  4. Caesar, H., Uijlings, J., Ferrari, V.: Coco-stuff: Thing and stuff classes in context. In: Proceedings of IEEE Conference on Computer Vision and Pattern Recognition (2018) [2](#), [6](#), [10](#), [18](#)
  5. Chen, Y.C., Li, L., Yu, L., El Kholy, A., Ahmed, F., Gan, Z., Cheng, Y., Liu, J.: Uniter: Universal image-text representation learning. In: Proceedings of European Conference on Computer Vision (2020) [3](#)
  6. Cheng, B., Misra, I., Schwing, A.G., Kirillov, A., Girdhar, R.: Masked-attention mask transformer for universal image segmentation. Proceedings of IEEE Conference on Computer Vision and Pattern Recognition (2022) [2](#), [4](#)
  7. Cheng, B., Schwing, A., Kirillov, A.: Per-pixel classification is not all you need for semantic segmentation. International Conference on Neural Information Processing Systems (2021) [2](#), [4](#)
  8. Cheng, X., Xiong, H., Fan, D.P., Zhong, Y., Harandi, M., Drummond, T., Ge, Z.: Implicit motion handling for video camouflaged object detection. In: Proceedings of IEEE Conference on Computer Vision and Pattern Recognition (2022) [5](#), [10](#), [14](#)
  9. Cherti, M., Beaumont, R., Wightman, R., Wortsman, M., Ilharco, G., Gordon, C., Schuhmann, C., Schmidt, L., Jitsev, J.: Reproducible scaling laws for contrastive language-image learning. Proceedings of IEEE Conference on Computer Vision and Pattern Recognition (2022) [2](#), [4](#), [11](#), [15](#)
  10. Cho, S., Shin, H., Hong, S., An, S., Lee, S., Arnab, A., Seo, P.H., Kim, S.W.: Catseg: Cost aggregation for open-vocabulary semantic segmentation. arXiv preprint (2023) [4](#), [10](#), [11](#), [14](#), [17](#), [18](#)
  11. Csurka, G., Volpi, R., Chidlovskii, B.: Semantic image segmentation: Two decades of research. Foundations and Trends in Computer Graphics and Vision (2022) [2](#)
  12. Everingham, M., Van Gool, L., Williams, C.K., Winn, J., Zisserman, A.: The pascal visual object classes (voc) challenge. International Journal of Computer Vision (2010) [2](#)
  13. Fan, D.P., Ji, G.P., Cheng, M.M., Shao, L.: Concealed object detection. IEEE Transactions on Pattern Analysis and Machine Intelligence (2021) [4](#), [5](#), [10](#)
  14. Fan, D.P., Ji, G.P., Sun, G., Cheng, M.M., Shen, J., Shao, L.: Camouflaged object detection. In: Proceedings of IEEE Conference on Computer Vision and Pattern Recognition (2020) [5](#), [14](#)
  15. Fan, D.P., Ji, G.P., Xu, P., Cheng, M.M., Sakaridis, C., Van Gool, L.: Advances in deep concealed scene understanding. Visual Intelligence (2023) [2](#), [4](#), [18](#)
  16. Fan, D.P., Zhou, T., Ji, G.P., Zhou, Y., Chen, G., Fu, H., Shen, J., Shao, L.: Inf-net: Automatic covid-19 lung infection segmentation from ct images. IEEE Transactions on Medical Imaging (2020) [4](#)
  17. Ghiasi, G., Gu, X., Cui, Y., Lin, T.Y.: Scaling open-vocabulary image segmentation with image-level labels. In: Proceedings of European Conference on Computer Vision (2022) [11](#)

18. Gu, X., Lin, T.Y., Kuo, W., Cui, Y.: Open-vocabulary object detection via vision and language knowledge distillation. In: International Conference on Learning Representations (2021) [9](#), [11](#), [13](#), [18](#)
19. He, K., Gkioxari, G., Dollar, P., Girshick, R.: Mask r-cnn. *IEEE Transactions on Pattern Analysis and Machine Intelligence* (Feb 2020) [2](#)
20. He, K., Zhang, X., Ren, S., Sun, J.: Deep residual learning for image recognition. In: Proceedings of IEEE Conference on Computer Vision and Pattern Recognition (2016) [11](#)
21. Ji, W., Li, J., Bian, C., Zhou, Z., Zhao, J., Yuille, A.L., Cheng, L.: Multispectral video semantic segmentation: A benchmark dataset and baseline. In: Proceedings of IEEE Conference on Computer Vision and Pattern Recognition (2023) [4](#)
22. Ji, W., Li, J., Zhang, M., Piao, Y., Lu, H.: Accurate rgb-d salient object detection via collaborative learning. In: Proceedings of European Conference on Computer Vision (2020) [4](#)
23. Ji, W., Yan, G., Li, J., Piao, Y., Yao, S., Zhang, M., Cheng, L., Lu, H.: Dmra: Depth-induced multi-scale recurrent attention network for rgb-d saliency detection. *IEEE Transactions on Image Processing* (2022) [4](#)
24. Jia, Q., Yao, S., Liu, Y., Fan, X., Liu, R., Luo, Z.: Segment, magnify and reiterate: Detecting camouflaged objects the hard way. In: Proceedings of IEEE Conference on Computer Vision and Pattern Recognition (2022) [5](#)
25. Katsuki, F., Constantinidis, C.: Bottom-up and top-down attention: different processes and overlapping neural systems. *The Neuroscientist* (2014) [8](#)
26. Kim, S.Y., Zhang, J., Niklaus, S., Fan, Y., Chen, S., Lin, Z., Kim, M.: Layered depth refinement with mask guidance. In: Proceedings of IEEE Conference on Computer Vision and Pattern Recognition (2022) [10](#)
27. Le, T.N., Nguyen, T.V., Nie, Z., Tran, M.T., Sugimoto, A.: Anabranch network for camouflaged object segmentation. *Computer Vision and Image Understanding* (2019) [5](#)
28. Li, A., Zhang, J., Lyu, Y., Liu, B., Zhang, T., Dai, Y.: Uncertainty-aware joint salient object and camouflaged object detection. In: Proceedings of IEEE Conference on Computer Vision and Pattern Recognition (2021) [5](#)
29. Li, G., Duan, N., Fang, Y., Gong, M., Jiang, D.: Unicoder-vl: A universal encoder for vision and language by cross-modal pre-training. In: AAAI Conference on Artificial Intelligence (2020) [3](#)
30. Li, J., Ji, W., Wang, S., Li, W., Cheng, L.: Dvsod: Rgb-d video salient object detection. In: International Conference on Neural Information Processing Systems (2023) [4](#)
31. Li, J., Ji, W., Zhang, M., Piao, Y., Lu, H., Cheng, L.: Delving into calibrated depth for accurate rgb-d salient object detection. *International Journal of Computer Vision* (2023) [4](#)
32. Li, X., Yin, X., Li, C., Zhang, P., Hu, X., Zhang, L., Wang, L., Hu, H., Dong, L., Wei, F., et al.: Oscar: Object-semantics aligned pre-training for vision-language tasks. In: Proceedings of European Conference on Computer Vision (2020) [3](#)
33. Liang, F., Wu, B., Dai, X., Li, K., Zhao, Y., Zhang, H., Zhang, P., Vajda, P., Marculescu, D.: Open-vocabulary semantic segmentation with mask-adapted clip. *Proceedings of IEEE Conference on Computer Vision and Pattern Recognition* (2022) [4](#), [10](#), [11](#), [14](#), [17](#), [18](#)
34. Lin, D., Dai, J., Jia, J., He, K., Sun, J.: Scribblesup: Scribble-supervised convolutional networks for semantic segmentation. *Proceedings of IEEE Conference on Computer Vision and Pattern Recognition* (2016) [18](#)

35. Litjens, G., Kooi, T., Bejnordi, B.E., Setio, A.A.A., Ciompi, F., Ghafoorian, M., van der Laak, J.A., van Ginneken, B., Sánchez, C.I.: A survey on deep learning in medical image analysis. *Medical Image Analysis* (2017) [2](#)
36. Liu, L., Wang, R., Xie, C., Yang, P., Wang, F., Sudirman, S., Liu, W.: Pestnet: An end-to-end deep learning approach for large-scale multi-class pest detection and classification. *IEEE Access* (2019) [4](#)
37. Liu, Z., Lin, Y., Cao, Y., Hu, H., Wei, Y., Zhang, Z., Lin, S., Guo, B.: Swin transformer: Hierarchical vision transformer using shifted windows. *Proceedings of the IEEE International Conference on Computer Vision* (2021) [11](#)
38. Liu, Z., Mao, H., Wu, C.Y., Feichtenhofer, C., Darrell, T., Xie, S.: A convnet for the 2020s. In: *Proceedings of IEEE Conference on Computer Vision and Pattern Recognition* (2022) [15](#)
39. Loshchilov, I., Hutter, F.: Decoupled weight decay regularization. In: *International Conference on Learning Representations* (2019) [10](#)
40. Lyu, Y., Zhang, J., Dai, Y., Li, A., Liu, B., Barnes, N., Fan, D.P.: Simultaneously localize, segment and rank the camouflaged objects. In: *Proceedings of IEEE Conference on Computer Vision and Pattern Recognition* (2021) [5](#)
41. McCrae, J.P., Rademaker, A., Fellbaum, C.D.: English wordnet 2019 – an open-source wordnet for english. In: *Global WordNet Conference* (2019) [15](#), [16](#)
42. Mithun, N.C., Panda, R., Papalexakis, E.E., Roy-Chowdhury, A.K.: Webly supervised joint embedding for cross-modal image-text retrieval. In: *Proceedings of the ACM International Conference on Multimedia* (2018) [4](#)
43. Mottaghi, R., Chen, X., Liu, X., Cho, N.G., Lee, S.W., Fidler, S., Urtasun, R., Yuille, A.: The role of context for object detection and semantic segmentation in the wild. In: *Proceedings of IEEE Conference on Computer Vision and Pattern Recognition* (2014) [2](#)
44. Neuhold, G., Ollmann, T., Bulò, S.R., Kotschieder, P.: The mapillary vistas dataset for semantic understanding of street scenes. In: *Proceedings of the IEEE International Conference on Computer Vision* (2017) [2](#)
45. Pang, Y., Zhang, L., Zhao, X., Lu, H.: Hierarchical dynamic filtering network for rgb-d salient object detection. In: *Proceedings of European Conference on Computer Vision* (2020) [4](#)
46. Pang, Y., Zhao, X., Xiang, T.Z., Zhang, L., Lu, H.: Zoom in and out: A mixed-scale triplet network for camouflaged object detection. In: *Proceedings of IEEE Conference on Computer Vision and Pattern Recognition* (2022) [5](#)
47. Pang, Y., Zhao, X., Xiang, T.Z., Zhang, L., Lu, H.: Zoomnext: A unified collaborative pyramid network for camouflaged object detection. *IEEE Transactions on Pattern Analysis and Machine Intelligence* (2024) [5](#)
48. Pang, Y., Zhao, X., Zhang, L., Lu, H.: Multi-scale interactive network for salient object detection. In: *Proceedings of IEEE Conference on Computer Vision and Pattern Recognition* (2020) [4](#)
49. Pang, Y., Zhao, X., Zhang, L., Lu, H.: Caver: Cross-modal view-mixed transformer for bi-modal salient object detection. *IEEE Transactions on Image Processing* (2023) [4](#)
50. Radford, A., Kim, J.W., Hallacy, C., Ramesh, A., Goh, G., Agarwal, S., Sastry, G., Askell, A., Mishkin, P., Clark, J., et al.: Learning transferable visual models from natural language supervision. In: *Proceedings of the International Conference on Machine Learning* (2021) [2](#), [4](#), [9](#), [11](#), [13](#), [14](#), [15](#), [18](#)
51. Ranftl, R., Bochkovskiy, A., Koltun, V.: Vision transformers for dense prediction. In: *Proceedings of the IEEE International Conference on Computer Vision* (2021) [10](#)

52. Rizzo, M., Marcuzzo, M., Zangari, A., Gasparetto, A., Albarelli, A.: Fruit ripeness classification: A survey (2023) [4](#)
53. Rombach, R., Blattmann, A., Lorenz, D., Esser, P., Ommer, B.: High-resolution image synthesis with latent diffusion models. In: Proceedings of IEEE Conference on Computer Vision and Pattern Recognition (2022) [11](#)
54. Skurowski, P., Abdulameer, H., Błaszczuk, J., Depta, T., Kornacki, A., Koziel, P.: Animal camouflage analysis: Chameleon database (2017), <http://kgwisc.aei.polsl.pl/index.php/pl/dataset/63-animal-camouflage-analysis> [5](#)
55. Su, W., Zhu, X., Cao, Y., Li, B., Lu, L., Wei, F., Dai, J.: Vi-bert: Pre-training of generic visual-linguistic representations. In: International Conference on Learning Representations (2019) [3](#)
56. Sun, Y., Wang, S., Chen, C., Xiang, T.Z.: Boundary-guided camouflaged object detection. In: International Joint Conference on Artificial Intelligence (2022) [7](#), [9](#)
57. Thisanke, H., Deshan, C., Chamith, K., Seneviratne, S., Vidanaarachchi, R., Herath, D.: Semantic segmentation using vision transformers: A survey. arXiv preprint (2023) [2](#)
58. Unal, O., Dai, D., Gool, L.V.: Scribble-supervised lidar semantic segmentation. Proceedings of IEEE Conference on Computer Vision and Pattern Recognition (2022) [18](#)
59. Vaswani, A., Shazeer, N., Parmar, N., Uszkoreit, J., Jones, L., Gomez, A.N., Kaiser, u., Polosukhin, I.: Attention is all you need. In: International Conference on Neural Information Processing Systems (2017) [7](#), [8](#)
60. Wu, J., Li, X., Xu, S., Yuan, H., Ding, H., Yang, Y., Li, X., Zhang, J., Tong, Y., Jiang, X., Ghanem, B., Tao, D.: Towards open vocabulary learning: A survey. arXiv preprint (2024) [2](#)
61. Xiang, M., Zhang, J., Lv, Y., Li, A., Zhong, Y., Dai, Y.: Exploring depth contribution for camouflaged object detection (2022) [7](#)
62. Xu, J., Liu, S., Vahdat, A., Byeon, W., Wang, X., De Mello, S.: Open-vocabulary panoptic segmentation with text-to-image diffusion models. In: Proceedings of IEEE Conference on Computer Vision and Pattern Recognition (2023) [4](#), [10](#), [11](#), [14](#), [18](#)
63. Xu, M., Zhang, Z., Wei, F., Hu, H., Bai, X.: Side adapter network for open-vocabulary semantic segmentation. Proceedings of IEEE Conference on Computer Vision and Pattern Recognition (2023) [2](#), [4](#), [10](#), [11](#), [14](#), [17](#), [18](#)
64. Xu, M., Zhang, Z., Wei, F., Lin, Y., Cao, Y., Hu, H., Bai, X.: A simple baseline for open-vocabulary semantic segmentation with pre-trained vision-language model. In: Proceedings of European Conference on Computer Vision (2021) [4](#), [10](#), [11](#), [14](#), [18](#)
65. Yang, J.: Plantcamo dataset (2023), <https://github.com/yjybuaa/PlantCamo> [5](#), [14](#)
66. Yang, L., Xu, X., Kang, B., Shi, Y., Zhao, H.: Freemask: Synthetic images with dense annotations make stronger segmentation models. In: International Conference on Neural Information Processing Systems (2023) [18](#)
67. Ye, H., Kuen, J., Liu, Q., Lin, Z., Price, B., Xu, D.: Seggen: Supercharging segmentation models with text2mask and mask2img synthesis. ArXiv (2023) [18](#)
68. Yin, B., Zhang, X., Hou, Q., Sun, B.Y., Fan, D.P., Van Gool, L.: Camoformer: Masked separable attention for camouflaged object detection (2022) [5](#), [9](#)
69. Yu, Q., Zhao, X., Pang, Y., Zhang, L., Lu, H.: Multi-view aggregation network for dichotomous image segmentation. In: Proceedings of IEEE Conference on Computer Vision and Pattern Recognition (2024) [4](#)

70. Yu, Q., He, J., Deng, X., Shen, X., Chen, L.C.: Convolutions die hard: Open-vocabulary segmentation with single frozen convolutional clip. In: International Conference on Neural Information Processing Systems (2023) [4](#), [10](#), [11](#), [14](#), [18](#)
71. Zabari, N., Hoshen, Y.: Open-vocabulary semantic segmentation using test-time distillation. In: European Conference on Computer Vision Workshops (2023) [4](#)
72. Zhang, M., Ji, W., Piao, Y., Li, J., Zhang, Y., Xu, S., Lu, H.: Lfnet: Light field fusion network for salient object detection. *IEEE Transactions on Image Processing* (2020) [4](#)
73. Zhang, M., Liu, J., Wang, Y., Piao, Y., Yao, S., Ji, W., Li, J., Lu, H., Luo, Z.: Dynamic context-sensitive filtering network for video salient object detection. In: Proceedings of the IEEE International Conference on Computer Vision (2021) [4](#)
74. Zhang, M., Yao, S., Hu, B., Piao, Y., Ji, W.: C2dfnet: Criss-cross dynamic filter network for rgb-d salient object detection. *IEEE Transactions on Multimedia* (2023) [4](#)
75. Zhang, W., Pang, J., Chen, K., Loy, C.C.: K-net: Towards unified image segmentation. *International Conference on Neural Information Processing Systems* (2021) [2](#)
76. Zhao, H., Puig, X., Zhou, B., Fidler, S., Torralba, A.: Open vocabulary scene parsing. In: Proceedings of the IEEE International Conference on Computer Vision (2017) [4](#)
77. Zhao, X., Chang, S., Pang, Y., Yang, J., Zhang, L., Lu, H.: Multi-source fusion and automatic predictor selection for zero-shot video object segmentation. *International Journal of Computer Vision* (2024) [4](#)
78. Zhao, X., Pang, Y., Ji, W., Sheng, B., Zuo, J., Zhang, L., Lu, H.: Spider: A unified framework for context-dependent concept understanding. In: Proceedings of IEEE Conference on Computer Vision and Pattern Recognition (2024) [4](#)
79. Zhao, X., Pang, Y., Zhang, L., Lu, H.: Joint learning of salient object detection, depth estimation and contour extraction. *IEEE Transactions on Image Processing* (2022) [4](#)
80. Zhao, X., Pang, Y., Zhang, L., Lu, H., Ruan, X.: Self-supervised pretraining for rgb-d salient object detection. In: AAAI Conference on Artificial Intelligence (2022) [4](#)
81. Zhao, X., Pang, Y., Zhang, L., Lu, H., Zhang, L.: Suppress and balance: A simple gated network for salient object detection. In: Proceedings of European Conference on Computer Vision (2020) [4](#)
82. Zhao, X., Pang, Y., Zhang, L., Lu, H., Zhang, L.: Towards diverse binary segmentation via a simple yet general gated network. *International Journal of Computer Vision* (2024) [4](#)
83. Zhao, X., Zhang, L., Pang, Y., Lu, H., Zhang, L.: A single stream network for robust and real-time rgb-d salient object detection. In: Proceedings of European Conference on Computer Vision (2020) [4](#)
84. Zheng, Y., Zhang, X., Wang, F., Cao, T., Sun, M., Wang, X.: Detection of people with camouflage pattern via dense deconvolution network. *IEEE Signal Processing Letters* (Jan 2019) [5](#), [14](#)
85. Zhou, B., Zhao, H., Puig, X., Fidler, S., Barriuso, A., Torralba, A.: Scene parsing through ade20k dataset. In: Proceedings of IEEE Conference on Computer Vision and Pattern Recognition (2017) [2](#), [6](#), [18](#)
86. Zhou, C., Loy, C.C., Dai, B.: Extract free dense labels from clip. In: Proceedings of European Conference on Computer Vision (2022) [4](#)

87. Zhou, H., Shen, T., Yang, X., Huang, H., Li, X., Qi, L., Yang, M.H.: Rethinking evaluation metrics of open-vocabulary segmentation. ArXiv [abs/2311.03352](#) (2023) [5](#)
88. Zhou, K., Yang, J., Loy, C.C., Liu, Z.: Learning to prompt for vision-language models. *International Journal of Computer Vision* (2021) [9](#), [11](#)
89. Zhu, C., Chen, L.: A survey on open-vocabulary detection and segmentation: Past, present, and future. arXiv preprint (2023) [2](#), [4](#), [10](#)
90. Zhu, F., Zhu, Y., Lee, V., Liang, X., Chang, X.: Deep learning for embodied vision navigation: A survey. arXiv preprint (2021) [2](#)